

Searching for interstellar quantum communications

Michael Hippke^{1,2}

¹*Sonneberg Observatory, Sternwartestr. 32, 96515 Sonneberg, Germany*  [@hippke](https://twitter.com/hippke)

²*Visiting Scholar, Breakthrough Listen Group, Berkeley SETI Research Center, Astronomy Department, UC Berkeley*

Abstract

The modern search for extraterrestrial intelligence (SETI) began with the seminal publications of [Cocconi & Morrison \(1959\)](#) and [Schwartz & Townes \(1961\)](#), who proposed to search for narrow-band signals in the radio spectrum, and for optical laser pulses. Over the last six decades, more than one hundred dedicated search programs have targeted these wavelengths; all with null results. All of these campaigns searched for classical communications, that is, for a significant number of photons above a noise threshold; with the assumption of a pattern encoded in time and/or frequency space. I argue that future searches should also target *quantum communications*. They are preferred over classical communications with regards to security and information efficiency, and they would have escaped detection in all previous searches. The measurement of Fock state photons or squeezed light would indicate the artificiality of a signal. I show that quantum coherence is feasible over interstellar distances, and explain for the first time how astronomers can search for quantum transmissions sent by ETI to Earth, using commercially available telescopes and receiver equipment.

Keywords: general: extraterrestrial intelligence, instrumentation: detectors, methods: data analysis

1. Introduction

The search for extraterrestrial intelligence (SETI) started in earnest with a discussion between Phil Morrison and his collaborator: “And Cocconi came to me one day and said, ‘You know what, Phil? If there are people out there, won’t they communicate with gamma rays that’ll cross the whole galaxy?’ And I said, ‘Gee, I know nothing about that (...) Why not use radio? It’s much cheaper. You get many more photons per watt and that must be what counts.’ And we began working on that and pretty soon we knew enough about radio astronomy to publish a paper called ‘Searching for Interstellar Communications.’” ([Gingerich 2003](#)). Morrison’s reason for radio, and against optical and γ -ray communication was that they “demand very complicated techniques”. However, only months later, the laser was invented ([Maiman 1960](#)). It was clear right away that the tighter beam of optical communication can increase the data rate compared to radio communications ([Schwartz & Townes 1961](#)), who write that “No such device was known a year ago”.

Since the 1960s, the vast majority of all SETI experiments have been done in the microwave regime. These search for narrow-band (Hz) microwave (GHz) signals (e.g., [Price et al. 2020](#)), and take into account

some amount of the unknown Doppler drift, typically $\pm 20 \text{ Hz s}^{-1}$ ([Sheikh et al. 2020](#)).

A smaller number of searches has been made in the optical. In the time domain, the signal assumption is a pulsed laser. Signal photons are expected to arrive in a pulse, e.g., 100 photons per square meter in one 1 ns bin, whereas starlight noise (with Poisson distribution) would only contribute few photons per nanosecond per square meter (e.g., [Howard et al. 2004](#); [Hanna et al. 2009](#); [Abeysekara et al. 2016](#)). In the frequency domain, the signal assumption is a continuous-wave narrow-band laser. Sun-like stars exhibit few natural spectral emission lines only at certain known wavelengths. Additional spectral emission lines, perhaps coinciding with known laser lines, could be artificial (e.g., [Reines & Marcy 2002](#); [Tellis & Marcy 2017](#); [Marcy 2021](#)).

The general search assumption is that of a beacon, i.e. a lighthouse in the sky: easy to find, but bearing little to no information. Isotropic beacons are most plausible in the microwave regime, because each photon is cheap, and large apertures can be made at low cost. For communications which aim to maximize the amount of data, however, shorter wavelengths are preferred because of their reduced free-space loss ([Hippke & Forgan 2017](#)). Such collimated beams, however, are rarely intercepted accidentally. Instead, it is much more likely to find signals deliberately directed at the Earth ([Forgan 2014](#)). They may originate from ETI on distant exoplanets, or from probes or repeater stations in the solar system neighborhood ([Hippke 2020](#)). As humans

are already actively communicating into space with radio and laser beams, it is insightful to examine how our own technology tackles interplanetary communications. Consequently, I will discuss examples of and proposals for human communications, under the assumption that some of these methods are replicated by putative ETI.

We are looking (and should keep looking) for narrow-band lighthouse blasts, even though we have found none yet. At the same time, it is possible to expand our search. What is today recorded as just starlight might in fact include a weaker, underlying signal, based on the foundation of quantum communications. It is sometimes argued in the hallways of astronomy departments that we “just have to tune into the right band” and – voilà – will be connected to the galactic communication channel. I make this hypothesis testable for starlight and quantum communications.

2. The case for quantum communications

I can offer four arguments why ETI will choose to transmit quantum communications instead of simple classical beacons: gate-keeping, supremacy, security, and information efficiency.

2.1. Gate-keeping

ETI may deliberately choose to make communications invisible for less advanced civilizations. Perhaps most or all advanced civilization feel the need to keep the “monkeys” out of the galactic channel, and let members only participate above a certain technological minimum. Mastering quantum communications may reflect this limit. The argument was first made by Subotowicz (1979) when discussing communication by neutrino beams, which he judged as “so difficult that an advanced civilization may purposely choose such a system in order to find and communicate only with ETCs at their own level of development”. Yet, only 33 years after Subotowicz, Neutrino communications have now been shown at a basic level (0.1 bits/s) in a practical experiment (Stancil et al. 2012). However, communication with Neutrinos has a multitude of practical disadvantages over photons, which makes them unattractive for any conceivable rational being (Hippke 2018a). In practice, quantum Neutrino communication is unrealistically difficult due to their small cross-section, which makes it virtually impossible to detect entangled pairs (Blasone et al. 2009). Other particles like the neutron are easier to detect, but prohibitively energetically costly to focus into tight beams (Table 1 in Hippke 2018a). It appears that photons are most suitable for classical *and* quantum interstellar communications. The quantum part, however, may serve as ETI’s gate-keeping.

2.2. Quantum supremacy

Quantum supremacy describes the capability of quantum computers to solve certain problems exponentially faster than classical computers. One example is Shor’s

algorithm, a method for factoring integers in polynomial time, rather than exponential time. How is this relevant for interstellar communications?

Classical computers were, at their beginning, isolated local objects. Konrad Zuse built the the first Turing-complete computer, the Z3, in his Berlin apartment in 1941. The first computer networks were established about three decades later, beginning with the ARPANET, in 1969. Today’s internet connects billions of devices over all of Earth, exchanging large amounts of classical data over classical channels. It is plausible to assume that future space exploration will expand such a network to the planets and the stars (Hippke 2020).

The rise of quantum computers (Arute et al. 2019; Zhong et al. 2020) paves the way for a similar expansion of the quantum internet (Caleffi et al. 2018). The necessary quantum interconnects can be built with optical interactions of photons and atoms, in order to distribute entanglement across a network and teleport quantum states between nodes (Kimble 2008). Connecting quantum computers over quantum networks allows to transmit qubits from one quantum processor to another over long distances. Possible applications include physics and chemistry simulations (Feynman 1982; Lloyd 1996), e.g. collider reactions or nitrogen fixation, as well as machine learning, in particular deep learning (Benedetti et al. 2016; Ajagekar & You 2020).

One difficulty for an interstellar quantum network is the delay from light travel time, which is at least several years, compared to a fraction of a second for Earth-based networks. Thus, it is plausible that most quantum computations are performed locally (e.g., the training of a quantum computing deep learning network), and only the condensed qubits are transmitted for remote application (e.g., inference). A second plausible application is optical interferometry for astronomy over arbitrarily long baselines. This is possible by recording the electromagnetic field’s amplitude and phase as a function of time. After transmission of a set of qubits to the other’s location, both datasets can be combined into one observation (Bland-Hawthorn et al. 2021).

It may be plausible that future humans, or ETI, build an interstellar quantum network, perhaps for the purpose of distributed quantum computing. This may sound exotic today, but humans have mastered radio telecommunications for only 100 years, and are already at the brink of the transition to quantum communications (Kumar et al. 2019; Manzalini 2020). After another hundred (or million) years of advancement, it will perhaps appear obvious to any civilization that every reasonable other civilization will have converged on the best solution (which is quantum) in almost no time. After all, it is likely that most civilizations are older and more advanced than ourselves (Kipping et al. 2020).

2.3. Information security

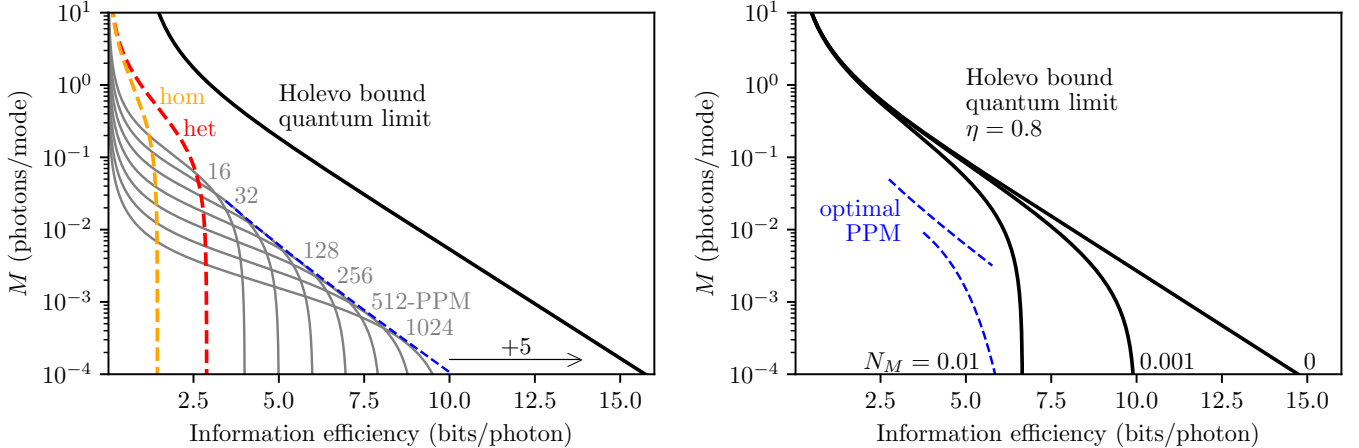


Figure 1. Photon information efficiency (PIE, in bits per photon) as a function of dimensional efficiency (DIE, in photons per mode). The area to the right of the Holevo bound, i.e. the quantum limit, is physically forbidden. *Left:* Homodyne (orange dashed) and heterodyne (red dashed) hit brick-wall limits of $\log_2(e) \sim 1.44$ and $2\log_2(e) \sim 2.89$ bits per photon even at infinite modes (infinite signal-to-noise ratio in classical terms). Pulse-position modulations (PPM) is shown in gray with modulations of different orders. The optimal order is approximated in blue (dashed). The gap in information efficiency between PPM and the quantum limit is about 50 %. All curves without noise and losses. *Right:* Holevo limit with receiver efficiency $\eta = 0.8$ and different noise levels (in photons per mode). PPM approaches the Holevo limit in the noise-limited case to within $1/\ln(2) \sim 1.44$ bits (see text).

A quantum channel can transport *classical* information, such as an encyclopedia, as well as *quantum* information, i.e., quantum bits (“qubits”). These can be used for secure transmissions with cryptography based on quantum key distribution. We do not know whether ETI values secure interstellar communication, but it is certainly a beneficial tool for expansive civilizations which consist of factions, like humanity today. Therefore, it is plausible that future humans (or ETI) have a desire to implement a secure interstellar network.

For this purpose, quantum key distribution is the method to implements a cryptographic protocol based on quantum mechanics. Its security relies on the foundations of quantum mechanics, which holds as long as the theory is correct. In contrast, traditional public key cryptography relies on the computational difficulty of certain mathematical functions, which may be broken with future technological advances such as quantum computers.

Quantum key distribution enables two distant parties to produce a shared secret key, which can be used to encrypt and decrypt subsequent messages. A unique property of quantum key distribution is the possibility of the two parties to detect a potential third party which intercepts the message. Based on quantum mechanics, the process of measuring a quantum system disturbs it, introducing detectable anomalies. Thus, a communication system can be implemented which detects eavesdropping. If no eavesdropping occurs, the channel is guaranteed to be secure. After key production and distribution, the actual message can be encrypted and transmitted over a classical (or quantum) channel.

The energy cost of secure quantum communications (Ding et al. 2017), and the capacity of the quantum-secure channel (Gagatsos et al. 2020) are active research areas.

2.4. Information efficiency

A quantum channel can deliver more classical information per unit energy than a classical channel. In other words, to achieve the highest number of bits per photon, i.e. to maximize the data rate, quantum communication is required. Turned the other way around, classical channels are energetically wasteful, because they do not use all information encoding options per photon.

It must explicitly be stated that there is no exponential gain in photon information efficiency (PIE, in bits per photon) possible through the use of many qubits in superposition. In quantum computing, a memory with n bits of information has 2^n possible states. This sometimes leads to the wrong statement that a quantum computer can save 2^n bits of information using n quantum logic gates (an exponential gain of quantum over classical). The correct statement is that n qubits can carry up to $2n$ bits of classical information (Holevo 1973) using super-dense coding (Bennett & Wiesner 1992).

A detailed summary of classical and quantum capacity, with and without noise, will be published elsewhere (Hippke 2021 in prep.). The interstellar use case is in the photon-starved regime, where the number of modes is much larger than the number of photons, $M \ll 1$. In the low noise case, the capacity of the classical channel is $\log_2(1/M) - \log_2(\log(1/M))$ bits per photon (Jarzyna et al. 2015; Banaszek et al. 2020). It can be

reached to within a few percent using simple schemes such as high-order pulse-position modulation (PPM). In contrast, the capacity of the quantum channel is $(1+M)\log_2(1+M) - M\log_2(M)/M + 1$ bits per photon (Giovannetti et al. 2004). Thus, the quantum advantage is $\log_2(1/M) + \log_2(e)$, which is 3–6 bits per photon for $10^{-3} < M < 10^{-23}$ (Figure 1). In other words, quantum communications can boost the number of bits per photon by up to $\sim 1/3$. In the noise-limited case, the advantage of quantum communications converges to $1/\ln(2) \sim 1.44$ bits per photon (König & Smith 2013).

A quantum advantage of order $1/3$ does not seem like much, but why waste it? It is logical to assume that ETI prefers to transmit more information rather than less, per unit energy. The only quantum “cost” is more complicated technology (although this point may be obsolete in a few decades, when quantum technology will have become trivial).

3. Coherence over interstellar distances

It was recently shown that quantum coherence of photons over interstellar distances is possible in principle (Berera 2020). As a baseline, the largest distance over which successful optical entanglement experiments have been performed on Earth is 144 km (Fedrizzi et al. 2009). The mass density of the Earth’s atmosphere at sea level is 1.2 kg m^{-3} . Integrated over a column of 144 km, the column density is $172,800 \text{ kg m}^{-2}$. Satellite-based quantum communications traverse smaller column densities on their combined up and down paths (Yang et al. 2019). Mass density in space is much lower, but the distances are much greater. Thus, we must examine the column density to the stars in order to determine the feasibility of interstellar quantum communications. This includes interplanetary and interstellar dust (grains) and gas (atoms).

A detailed analysis will be published elsewhere (Hippke 2021 in prep.). In brief, the largest contributors to decoherence are interplanetary dust, mainly produced by mass loss from comets and asteroids, or by fragmentation of meteoroids; it is concentrated mainly in the ecliptic plane. Particles are present in the form of atomic hydrogen, helium, and free electrons; they originate from the solar wind and from interstellar flow. The combined interplanetary and interstellar column density between the Earth and the nearest star, Proxima Centauri, is about $3 \times 10^{-8} \text{ kg m}^{-2}$ (Mann & Kimura 2000). This is 8 orders of magnitude less than the 144 km through Earth’s atmosphere. The atmospheric influence on decoherence dominates for all distances $< \text{kpc}$ and all wavelengths except those in the Lyman continuum ($\approx 50 - 91 \text{ nm}$) which is opaque even for the closest stars due to the ionization of neutral hydrogen (Barstow & Holberg 2007).

4. Quantum communication implementations

If quantum is the way to go, what do quantum communications look like? What do we need to search for?

There are three cases to consider. Either the transmitter uses quantum building blocks, or the receiver, or both. For quantum cryptography, i.e. secure communications, both ends need to be quantum. To transmit the maximum amount of classical information over a quantum channel, i.e. to achieve the Holevo bound, only one side requires quantum methods (Hausladen et al. 1996; Schumacher & Westmoreland 1997; Holevo 1998). With our current technological understanding, it is unclear which side is easier to implement. If a quantum transmitter is difficult to build, it would be advantageous to use a classical coherent light source (a laser) and let the receiver do the quantum lift. On the other hand, if pair photons can readily be made, e.g., with semiconductor quantum dots (Santana et al. 2017), they could be used onboard a spacecraft.

Quantum communications based on photons can be realized with several known physical implementations, or combinations thereof. The first is polarization encoding, where the horizontal and vertical polarization of light is used. The second is through the number of photons (their Fock state), where either an integer number of photons is present, or vacuum. The third option is time-bin encoding, where the time of arrival (early or late) is used. The fourth option is a coherent state of light, known as squeezed light. Here, the information support is quadrature (amplitude-squeezed or phase-squeezed state). Finally, instead of a two-level system, one can use larger dimensional systems such as orbital angular momentum (OAM). At the cost of larger spatial divergence, multiple photons can encode several bits of information using OAM.

In comparison, classical communications in the low M regime most commonly use on-off keying (or pulse-position modulation in the strong-loss regime), which is the simplest form of amplitude shifts. Simplified, the presence or lack of a carrier (a photon) signifies a binary one or zero. Less commonly, binary digits are encoded on the wavelength of a photon or on its polarization.

4.1. Quantum transmitter

The first option for a quantum communication scheme is a transmitter using quantum light, paired with a classical receiver. As Giovannetti et al. (2004) put it, “number-state systems for the lossless channel require a non-classical light source, but its receiver can use simple modal photon counting”. This also applies to the lossy bosonic channel; e.g., photons with free-space loss (Wilde et al. 2012; Oi et al. 2013).

The most common form of nonclassical light is the usage of Fock states: a quantum state with a well-defined number (an exact number) of particles (quanta), here: photons. A single-mode system in the Fock state $|n\rangle$ contains exactly n excitations of energy, in multiples of Planck’s constant \hbar . Such a Fock-state photon transmitter could be paired with a classical receiver, counting the specific photon numbers classically, which would achieve

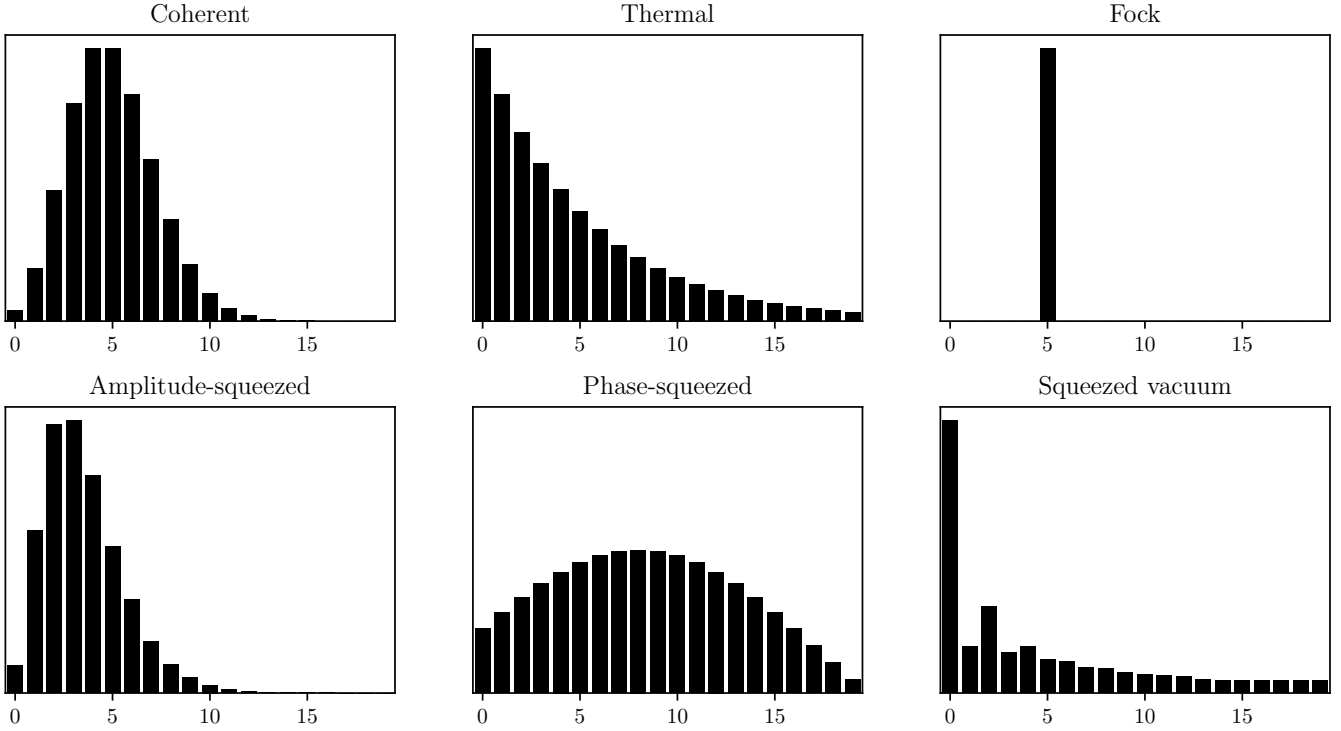


Figure 2. Photon number distributions for different states of light. The horizontal axis shows the number of photons per unit time, the vertical axis is in arbitrary units. Coherent (laser) light has different temporal bunching compared to thermal light, which is strictly decreasing in the number of photons per unit time. An idealized Fock state with 5 photons is shown in the upper right panel. The amplitude-squeezed state has a denser distribution compared to laser light, while the phase-squeezed state appears wider. The (pure) squeezed-vacuum state is special because it has no contribution from odd-photon-number states.

the Holevo limit. As the number of photons is affected by quantum uncertainty (following a Poisson distribution), the Fock states improve number state statistics, allowing to surpass the classical Shannon limit. Simplified, classical light comes with a probability in the number of photons per pulse. In a Fock state, this probability is tighter (Figure 2), reducing uncertainty for the receiver about what symbol was detected, and thus increasing capacity (Guerrini et al. 2019).

Similar schemes are possible using squeezed light (Müller et al. 2018). A useful analogy is Binary Phase Shift Keying (BPSK), where phase-squeezed light provides tighter phase uncertainties (Vourdas & da Rocha 1994; Fanizza et al. 2020). From an information perspective, a classical receiver would be sufficient for a perfect measurement, because the heavy lifting is done on the transmitter side. From an OSETI perspective, the measurement of Fock state photons or squeezing would indicate the artificiality of a signal.

4.2. Quantum receiver

Alternatively, the transmitter can use classical light, e.g., coherent laser light, while the quantum lifting is done on the receiver end. As Giovannetti et al. (2004) put it, a “coherent-state system uses a classical transmitter, but its detection strategy can be highly non-classical.”

While a classical receiver counts each photons and destroys it during the measurement, a quantum receiver must measure an ensemble of photons jointly before their destruction; the device is thus called a joint-detection receiver. No such device has been built yet, but there exist construction proposals and laboratory experiments.

With a transmitter sending classical laser light, and the receiver performing the quantum uplift, we can already search for such transmissions – they are “only” laser light. When recorded classically (neglecting the quantum receiver), the decoding of the message would remain impossible. The character of the transmission as laser light, however, can prove its artificiality. Still, I will briefly summarize quantum receivers to provide some insights into the future of quantum communication detectors.

At first, it might appear illogical that classical laser light can be paired with an improved (quantum) receiver to generate a higher information efficiency – after all, where should the additional bits per photon come from? The correct mental image here is that the transmitter indeed sends “only” classical light, but with the corresponding classical error probability for each bit. Due to the quantum nature of light, classical communication is not perfect and error-free. Instead, its coding scheme is optimized in such a way that probability of error (for

each bit, symbol, message) is below some threshold. Now, a better measurement reduces the measurement errors, allowing for denser coding.

Indeed, some of the first laboratory implementations which surpass the classical Shannon limit are benchmarked with respect to the [Helstrom \(1976\)](#) limit. For example, [Becerra et al. \(2015\)](#) describe a receiver which discriminates among four possible quadrature phase shift keying (QPSK) states, using a 99:1 beamsplitter, local oscillator, and a photon counter.

Collecting many photons before their destructive measurement is challenging. One method might be a “slicing receiver” for Fock-state photons ([da Silva et al. 2013](#)) which discriminates between any set of coherent state (laser light) signals using a small all-optical special-purpose quantum computer. The quantum computer must be able to do arbitrary logic on a set of qubits.

A related scheme uses the concept of Hadamard sequences of input symbols (BPSK at the transmitter side) that are mapped by a linear optical transformation from BPSK onto the PPM format by the quantum receiver ([Guha 2011](#)). The receiver would need to use quantum memories for collective readout of the classical information ([Klimek et al. 2016](#)). Instead of a real quantum memory (which is an area of active research), one could emulate it with known components. To perform collective measurements over multiple time bins requires the synchronization of individual incoming pulses at the receiver, while retaining mutual phase relations. To achieve this with standard tools, one could use fast optical switches and delay lines to equalize pulse arrival times before the Hadamard circuit. However, the whole ensemble grows quickly in size. For a PPM sequence of order 8, the same number of [Dolinar \(1973\)](#)-receivers are required, located behind a matrix of $8 + 7 + 6.. + 1 = 36$ beamsplitters of various transmission coefficients, and a similar number of phase shifters (Figure 2 in [Klimek et al. 2016](#)). As explained in section 2.4, the interesting regime for interstellar communications lies in the low- M region, requiring large ($> 10^3$) PPM orders. Such receivers are impractical to build with physical devices like beamsplitters because of the complexity, size, and transmission losses involved. Instead, quantum computers with quantum memory are preferable.

4.3. Pre-shared entanglement

[Bennett et al. \(2002\)](#) proved that pre-shared entanglement increases the capacity of a channel. This scheme is attractive for the use-case of a space probe which launches from the Earth, and takes onboard a box of particles later used to improve data transfer. As explained in the introduction, this is a communication scenario based on human imagination. Communications from ETI may, or may not, leverage similar principles.

First of all, this physically correct and feasible scheme must be distinguished from incorrect descriptions in the literature. Faster-than-light communication using quan-

tum entanglement is a common theme in science fiction (e.g., [Cline 2015](#)). In some realizations, two distant parties possess a box of entangled particles. They can “set” particles in such a way that the other side can then make a measurement, and immediately obtain the information. This is unphysical because faster-than-light signalling results in causality violations which are impossible to accept ([Eberhard & Ross 1989](#); [Bassi & Ghirardi 2008](#); [Ghirardi & Romano 2012](#); [Filatov & Auzinsh 2020](#)).

But what about a storage of entangled particles, with light-speed information exchange? Alice sends a box of particles to Bob onboard a spaceship. Bob opens the box and “modifies” the quantum states; the entangled partner particle in Alice’s box would take the same state, allowing for bits to be communicated – after some wait time covering for the light travel time. This idea is equally unphysical. It is prohibited by the no-communication theorem ([Croke et al. 2008](#)): through measurement of an entangled quantum state, it is not possible for one party to communicate information to another party. The fundamental misunderstanding about entanglement is that it only works when measuring the particle’s state. If Bob forces his entangled particle into a particular state (+1 or -1), the entanglement is broken. Alice’s subsequent measurement of her previously entangled particle, light years away, will now be +1 or -1 at random chance.

In contrast, the scheme by [Bennett et al. \(2002\)](#) is correct. Simplified, Alice performs some superoperator on her half, using a pre-shared qubit and a classical bit of data. She then sends the tensor product through the channel, which Bob can use to decode with the help of his half of the pre-shared information. In other words, the pre-shared information can be used to “compress” information. The scheme is, in fact, very similar to “normal” quantum communication with a combination of entanglement and separately sent classical information (e.g., [Hao et al. 2021](#)). The only difference is that the entangled part was shared before the start of the communication.

The gain from pre-sharing is an active research area. In the (theoretical) case of an infinitely large pre-shared cache, and no losses or noise, there is an “infinite-fold enhancement in communications capacity using pre-shared entanglement” ([Guha et al. 2020](#)). Numerically, even an infinite cache only increases the channel capacity (in bits per photon) by $C_E/C = \ln(1/M)$. For $M = 10^{-4}$, the increase is at most $\sim 9.2\times$. In practice, noise and losses eat quickly into this gain and reduce it to a factor of about two or less in all realistic cases.

On a starshot-like probe, the entangled caches would need to withstand decoherence for decades. For this purpose, quantum memory for entangled photons ([Saglamyurek et al. 2011](#)) can be used. The current (2021) world-record achieves a six-hour coherence time ([Zhong et al. 2015](#)), “made on a ground-state hyperfine transition of europium ion dopants in yttrium orthosilicate using optically detected nuclear magnetic resonance

techniques”. Such equipment is not yet suitable to take onboard of a tiny spacecraft, and is in any case insufficient. On the other hand, it is difficult to predict how tomorrow’s technology may inhibit decoherence over long times. One advantage for probes is that space is cold and dark, both factors which slow down decoherence.

The concept of Bennett et al. (2002) is a pre-shared entanglement communication protocol applicable to a communication from a spacecraft to its launch point. We may consider the observational signature for the case where Earthlings would intercept such a communication between an alien spacecraft and its home base. This observational signature would be identical to a *classical* transmission: The quantum lifting is performed before the two parties separated, and when merging their photons with their pre-shared particles (which we would not possess). Such a communication is not detectable by SETI experiments by its quantum signature. Instead, a SETI experiment would record classical (e.g., laser) communication. Earthlings would lack the required pre-shared entanglement photons to decipher the message. Without them, the classical transmission would appear random in nature. We could only guess that pre-shared entanglement is missing, and that humans are not the intended receiver. That case would imply the existence of at least two communicating parties other than humans.

5. Signatures and tools

Existing telescope facilities, including those performing optical SETI experiments, are not equipped with quantum communication receivers, because they do not yet exist. However, they often have at their disposal high-quality equipment to detect single photons, take spectra, and perform polarization experiments. I will show that such tools are sufficient to determine the presence of certain quantum communications. Therefore, we can proceed with methods that destroy the actual information content, as long as they provide us with indications of (lost) entanglement. A practical search will be complicated by the fact that we can not know the real characteristics of ETI signals, such as the actual encoding mode and the wavelength. Thus, SETI scientists will have to try many things, just as with today’s searches for classical signals. This opens up a whole new field of *Quantum SETI*.

5.1. Limitations of classical optical SETI

This section proves that current optical SETI experiments can only detect beacon-type signals, but miss communication links weaker in intensity than stars of the first magnitude. I will then describe how to detect such communication links by their quantum effects.

Standard OSETI experiments have a typical minimum sensitivity of order tens of photons per square meter per nanosecond (Maire et al. 2019) for cadences of order nanosecond (Table 1). Depending on the point of view, this limit can be regarded as astonishingly tight, or

terribly loose. It is loose when comparing it to the flux from a Sun-like (G2V) isotropic radiator,

$$F \sim 32 \text{ ns}^{-1} \text{ m}^{-2} \left(\frac{L}{L_\odot} \right) \left(\frac{1 \text{ pc}}{d} \right)^2. \quad (1)$$

Nominally, when pointing classical OSETI experiments even at bright stars, they will detect nothing, despite many photons hitting the detector (millions per second). On the other hand, when using tight transmitter beams, tight flux limits can be obtained. With a transmitter aperture of $A_t = 10 \text{ m}$, a receiver $A_r = 1 \text{ m}$, and $\lambda = 1 \mu\text{m}$ we get a flux of (Hippke & Forgan 2017)

$$F \sim \left(\frac{1 \text{ pc}}{d} \right)^2 \left(\frac{A_t}{1 \text{ m}} \right)^2 \left(\frac{A_r}{1 \text{ m}} \right)^2 \left(\frac{1 \mu\text{m}}{\lambda} \right) \left(\frac{P}{1 \text{ kW}} \right) (\text{s}^{-1}). \quad (2)$$

With a phased (unfilled) array of $A_r = 1,000 \text{ m}$ and $P = 30 \text{ MW}$, the received flux is sufficient to outshine Alpha Cen continuously. A km-sized phased aperture was proposed for “Breakthrough Starshot” (Lubin 2016a; Merali 2016; Popkin 2017) to propel a 1 g “space-chip” with 100 GW of laser power to $v = 0.2c$ in minutes. Aimed at Alpha Cen, this beamer would appear as a star of magnitude -4 on its sky, comparable to Venus and visible in daylight (Lubin 2016b). Even a $P = 30 \text{ MW}$ beam, undetected by OSETI experiments, can encode a lot of data. As an example, consider a perfect optical receiver at the time-bandwidth limit, e.g., a photon counter with $3 \times 10^{14} \text{ Hz}$. At a flux rate of $32 \times 10^9 \text{ s}^{-1}$, the number of photons per mode is $M = 10^{-4}$. From the Holevo limit, we find $\text{PIE} = \log_2(1/M) - \log_2(\log(1/M)) \sim 8$ bits per photon. With a 8192-ary PPM-type modulation, the frame duration would be $3 \times 10^{-10} \text{ s}$ and contain on average one signal photon. Then, the data rate is bound to about 256 Gbits/s. The second-order correlation function of the PPM modulation would appear with strong anti-bunching (Figure 4); I will discuss the detection of such signals in section 5.5.

An important issue with any interstellar communication (classical or quantum) is the free-space loss. The stated data rate, based on a PIE value and Equation 2, is only achievable for parameters exceeding the minimum requirements. A distant ETI signalling towards Earth, however, can not know our receiver’s aperture size. It must compensate for this by guessing a minimum size, and choosing its power level sufficiently high. Classical communication would transmit a series of PPM-pulses, each of e.g., kJ power, worth 10^{23} photons. On the receiver end, only a few of these photons would be received. For quantum communications, a protocol which requires the reception of a large fraction of photons would thus be inviable. Only quantum communication methods which can handle a large geometric loss are applicable. One of these could employ squeezed light, where each photon has quantum properties, but the information can be spread over many transmitted photons, as with pulses

Table 1. Pulsed OSETI detectors with published sensitivity limits

Observatory	Cadence (ns)	λ (nm)	Sensitivity ($\gamma \text{ m}^{-2} \text{ ns}^{-1}$)	Reference
Lick 1 m Nickel	5	450...850	51	Wright et al. (2001)
Harvard Oak Ridge 1.5 m	5	450...650	100	Howard et al. (2004)
Princeton Fitz Randolph 0.9 m	5	450...850	80	Howard et al. (2004)
STACEE heliostats	12	300...600	10	Hanna et al. (2009)
Leuschner 0.8 m	5	300...700	41	Korpela et al. (2011)
Harvard 1.8 m	5	300...800	60	Mead (2013)
Lick 1 m NIROSETI	1	950...1650	40	Maire et al. (2014)
Veritas 12 m	50	300...500	1	Abeysekara et al. (2016)
Boquete 0.5 m	5	350...600	67	Schuetz et al. (2016)

in PPM-like codes. Squeezed light is available today at 20 W power levels using parametric down-conversion (Aasi et al. 2013).

The discovery situation is not much better for spectral OSETI experiments. The usual search paradigm here is that laser light is very narrow-band; broadened to about 0.006 nm through atmospheric effects (Marcy 2021). For Holevo-bounded communication, however, narrow-band is not a valid assumption. For time-bandwidth limited pulses with central wavelength λ_0 and a spectral width (FWHM) $\Delta\lambda$, the pulse duration is approximately

$$\Delta t_{\min} = \frac{\lambda_0^2}{2 \Delta\lambda c} \quad (3)$$

with c as the speed of light. As an example, a near-infrared laser pulse with $\lambda = 1 \mu\text{m}$ with a $\Delta t_{\min} \sim 3 \times 10^{-14} \text{ s}$ requires a 5% bandwidth, i.e. $\Delta\lambda = 50 \text{ nm}$. Such a laser would be undetected by spectral searches.

This completes the point that OSETI experiments can find beacon-type pulses and laser lines, but no continuous communication signals, even when these are as powerful as first magnitude stars. It also opens the question: how do we detect strong laser-like communication signals?

5.2. Fast photon counters and time-bin encoding

The best option to detect time-bandwidth limited optical free-space communications would be to use a femtosecond photon counter, which would directly show the coherence of the photon arrival time stamps. Unfortunately, these have not yet been invented. The fastest photon detectors today have a timing jitter of 2.6 ps (i.e., $2.6 \times 10^{-12} \text{ s}$) in the optical, based on superconducting nanowires (SNSPDs, Korzh et al. 2020). Technology improved by about one order of magnitude per decade (Beskin et al. 1997; Tosi et al. 2009; Polyakov 2013). For comparison, the MANIA experiment used 100 ns counters in the 1980s (Shvartsman 1981), improving to a few ns in the 2000s (Wright et al. 2001). If progress continues in the same pace, we may possess sufficiently fast detectors in about 20 years.

Until then, we need to use other methods. An experiment with SNSPDs can explore the limits set by

atmospheric turbulence already today: optical and NIR laser pulses are smeared to $\Delta t \approx 10^{-12} \text{ s}$ (Hippke 2018b). At the time-bandwidth limit, their spectral width would be $\Delta\lambda \approx 1.5 \text{ nm}$. These pulses can already be time-resolved. A useful optical SETI experiment would be to time-tag incoming photons with ps accuracy using precise high time-resolution photon counters (Gol'tsman et al. 2001; Prochazka et al. 2013). Time-based correlations can be determined in post with data analysis, such as Fourier transforms and autocorrelation functions, building on the proposal by Leeb et al. (2013) and Stanton (2019). These experiments can test incoming sources (e.g., starlight) for the presence of time-bin encoding, which is one way of encoding the quantum information.

5.3. Laser warners and phase coherence

Defense forces try to solve a problem similar to OSETI. While we assume that ETI uses lasers to send signals across space, lasers on Earth are used by the military for targeting, range finding, and missile control. Laser warner receivers have been developed to detect the threat associated with incoming lasers. They use one or several of the following properties of coherent light: high brightness in a narrow spectral band, tight spatial beams, and phase coherence (Benton et al. 2019). In an interstellar setting, where the transmitter is far and small, it appears unresolved. Then, only temporal (pulsed) and spectral (narrow-band) properties remain, together with phase coherence.

To detect the presence of coherent light in the presence of noise (chaotic starlight, atmospheric noise etc.), it was already suggested by Kingsley (1993) to employ heterodyne and homodyne detection. A recent proposal by Benton (2019) proposes a method for a photon-counting laser coherence detection system. Based on an asymmetric Mach-Zehnder interferometer, it is equally sensitive to pulsed and continuous signals. For a wide spectral coverage, many sensors are required (e.g., 1024 APD cells for the same number of 1 nm wide frequency bins). Such a detector will be much more sensitive to the information bearing transmissions described in section 5.1, because it drops the requirement of a beacon-type threshold per

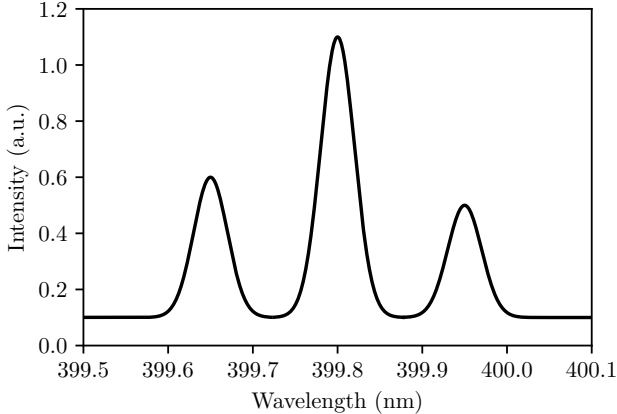


Figure 3. Synthetic spectrum expected from a laser with time-bin encoded qubits. Compared to a classical single frequency signal, three peaks occur, caused by the temporal modulation of the laser. Illustration based on Figure 3 in Donohue et al. (2013).

unit time, and instead integrates over arbitrary durations using Fourier transformation during post-processing.

5.4. Spectral encodings

Classical optical SETI also searches for narrow-band laser lines (e.g., Tellis & Marcy 2017). The assumption is that sun-like stars exhibit few natural spectral emission lines only at certain wavelengths. Thus, after removing known features, any remaining spectral peak could be a laser beam. In these classical searches, the expectation is to find a single peak narrow in frequency, as produced by continuous wave lasers (Reines & Marcy 2002).

Quantum communication signals, however, would be expected to be modulated in order to transport information. Plausible time-bandwidth limits are of order ps and tens of nm (section 5.1). Depending on the exact quantum encoding, there could be *three* spectral peaks separated by ~ 1 nm and of slightly different amplitude (Figure 3). Using existing data, one could examine spectra of stars for such multimodal emission features. Instead of a single emission line, quantum optical SETI would search for a frequency comb. Spectra could also be Fourier transformed to search for time-bin encoded signals (Hippke 2019).

5.5. Bunching: Hanbury Brown and Twiss effect

Photon (anti-)bunching is an (anti-)temporal correlation in the arrival time of subsequent photons, also known as the Hanbury Brown and Twiss effect (Brown & Twiss 1954). It is leveraged in astronomy for intensity interferometry (Hanbury Brown 1956). In the original experiment, two telescopes separated by a few meters were aimed at the star Sirius. Each telescope used a photon detector, and a correlation in the arrival time between the two fluctuating intensities was detected. The

correlation vanished when the distance between the telescopes was increased. This information can be used to determine the apparent angular size of the star.

There are three regimes of temporal photon correlations. The first is chaotic starlight with a blackbody-like spectrum, which exhibits positive bunching that is super-Poissonian distributed (Figure 4). In essence, photons arrive bunched (or clustered) in time. With a time difference τ between subsequent photon detections, one can define the first-order correlation function as $g^{(1)}(\tau)$, and the second order correlation function as

$$g^{(2)}(\tau) = 1 + |g^{(1)}(\tau)|^2. \quad (4)$$

Thermal blackbody radiation is the textbook example of $g^{(2)}(\tau) = 2$ (Glauber 1963; Saleh et al. 1991). Coherent laser light, i.e. light of a single frequency, shows as $g^{(2)}(\tau) = 1$. It follows the well-known Poissonian distribution. Finally, anti-bunching with $g^{(2)}(\tau) < 1$ has no classical wave analogue; its distribution is sub-Poissonian. In the limit of perfect anti-bunching, $g^{(2)}(\tau) = 0$, the arrival time between photons is constant. As a signal hypothesis, any $g^{(2)}(\tau) < 2$ from starlight indicates an artificial component. Anti-bunching ($g^{(2)}(\tau) < 1$) would be a strong indication of an information bearing signal based on pulse-position encoding schemes (section 5.2)

In practice, determining $g^{(2)}(\tau)$ for optical light is difficult. The coherence time of optical light near the time-bandwidth limit (10^{-14} s) is shorter than the best photon counters (10^{-12} s). The insufficient timing resolution causes extra noise which requires averaging many signals. Photon bunching was observationally shown for sunlight with a result of $g^{(2)}(\tau) = 1.45 \pm 0.03$ (Tan et al. 2014), and $g^{(2)}(\tau) = 1.7$; lower than the expected value of 2 due to noise. The same measurement was successfully performed with starlight (Tan & Kurtsiefer 2017) for stars such as P Cygni with a 1 m telescope, as well as β Canis Majoris and ϵ Orionis with the Veritas telescope (Abeysekara et al. 2020). In all cases, a significant value for $g^{(2)}(\tau) > 1$ was found. A signal-to-noise ratio discussion for starlight is given in Saha (2019). Similar experiments should be expanded to interesting targets listed in Lacki et al. (2020). A measurement of $g^{(2)}(\tau) < 1$ would constitute the discovery of quantum communications. The width of the invisible quantum emission line $\Delta\lambda$ (which could shift during the observation, $\lambda_0 \neq \text{const.}$) can be determined through the relation $\tau = \lambda_0^2/c\Delta\lambda$.

5.6. Hong-Ou-Mandel interference test

Another possibility is the Hong-Ou-Mandel interference test (Hong et al. 1987). This experiment is a two-photon interference effect only explainable with quantum optics. It only requires one 50 % beamsplitter and two photon counters at its outputs. Chaotic light, e.g., starlight, exhibits distinguishable properties: random polarizations, arrival times, and different wavelengths.

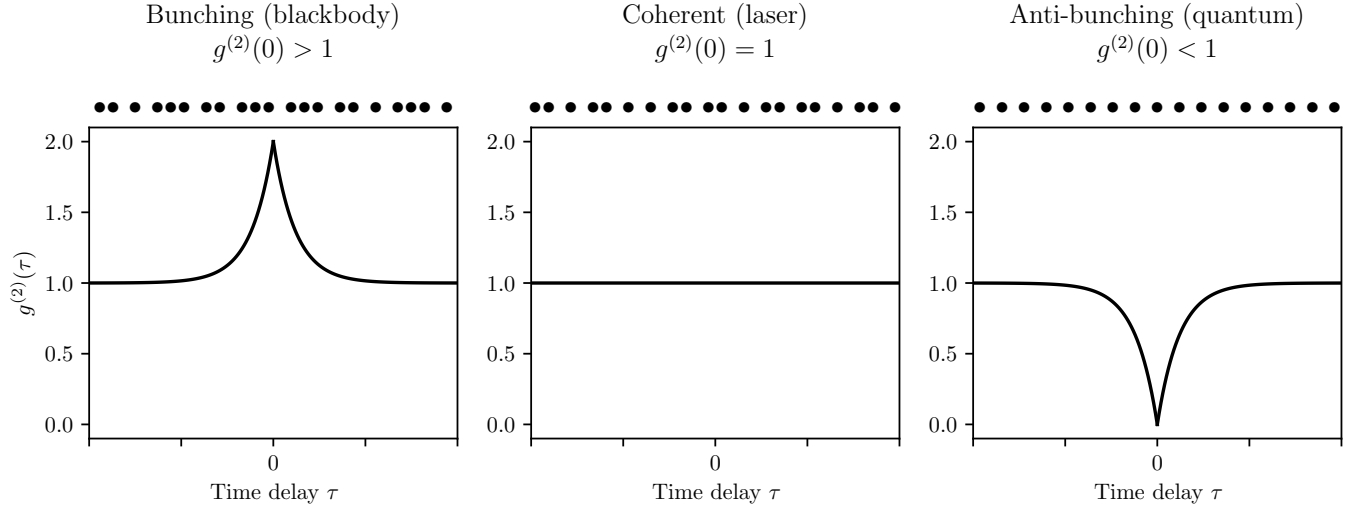


Figure 4. Temporal bunching of photons for super-Poisson distributed chaotic thermal starlight (left), Poisson-distributed coherent laser light (middle) and equally spaced (anti-bunched) quantum light. Cases where $g^{(2)}(0) < 2$ may be indicative of a mixture of starlight and artificial signals. For $g^{(2)}(0) < 1$ a quantum component is present.

These photons will then pass through the beamsplitter randomly and are registered by the detectors. When two distinguishable photons enter the beamsplitter, four possibilities arise with equal probabilities: both photons are transmitted, both photons are reflected, the photon coming in from the first end is reflected and the other transmitted, and the opposite of that.

In the case a pair of *indistinguishable* photons enters the beamsplitter, a quantum phenomenon occurs. Then, both photons will pass through to one of the sides: one photon counter will count two photons, the other photon counter will count zero photons. While this can also happen by 50 % chance for chaotic light, it will *always* happen for indistinguishable photons.

This experiment has been performed with sunlight and light created on the Earth (Deng et al. 2019). Despite the large physical separation of both sources, when filtered so that the photons become indistinguishable, they exhibit the quantum interference and allow for entanglement tests.

The signal hypothesis for a quantum SETI experiment, based on the Hong-Ou-Mandel interference test, would be as follows. A transmission would consist of a large number of indistinguishable photon pairs. Each pair might be distinguishable from other pairs in frequency, polarization, and arrival time; so that their integrated sum may look natural (e.g., replicate a blackbody spectrum). The signal, however, might partially or totally consist of indistinguishable photon pairs. One method to produce such pair photons are semiconductor quantum dots (Santana et al. 2017). An OSETI experiment could use two optical telescopes, focusing their light into each side of a beamsplitter. Through data analysis, one would find a pair ratio exceeding 50 % (noise and signal photons combined) in case an artificial signal fraction is the

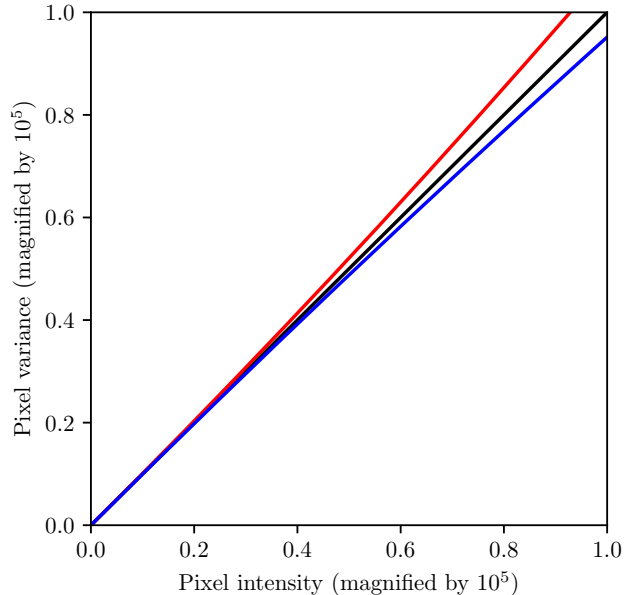


Figure 5. Signature of squeezed light on a CCD. Pixel variance as a function of pixel intensity for coherent light (laser, black, straight line), squeezed light (red), and anti-squeezed light (blue). Both quadratic functions are shown with coefficients enlarged by 10^5 for clarity.

experiment. In practice, the experiment requires very low-noise photon detectors, but is realistically possible at least for the brightest stars, as shown by Deng et al. (2019).

5.7. Squeezed light

Due to the uncertainty principle, a measurement of the amplitude of the light field delivers values within

an uncertainty region. Coherent states have circularly symmetric uncertainty regions. The uncertainty relation requires some minimum noise amplitudes for the amplitude and phase. Reducing either amplitude or phase uncertainty, at the expense of the other, constitutes “squeezed light” (Schnabel 2017).

First produced by degenerate parametric down conversion in an optical cavity (Wu et al. 1986), squeezed light can be made by using optical nonlinear interactions, such as frequency doubling, with the Kerr nonlinearity in optical fibers, or by atom-light interactions. Semiconductor lasers can produce amplitude-squeezed light when operated with a stabilized pump current. A famous application is in quantum metrology (Giovannetti et al. 2006) by the Laser Interferometer Gravitational-wave Observatory (LIGO), where a sub-threshold optical parametric oscillator produces a squeezed vacuum state (Aasi et al. 2013). It allows to improve detector noise performance at certain frequencies by a factor of a few, and makes the detection of gravitational waves from merging black holes, and other sources, possible (Abbott et al. 2016).

Squeezed light is not expected to occur from natural astrophysical processes. We may assume, however, that ETI signals leverage squeezing to maximize data rate of transmissions. As outlined in section 2.4, squeezed light can be used to achieve the Holevo bound of maximum photon information efficiency.

To test the presence of squeezed light, various methods are available. Most commonly, homodyne or heterodyne detection by beating the squeezed light field with a classical local oscillator is used. Other options are direct intensity detection or photon counting (for intensity-squeezed light only), or with a phase-shifting cavity (Vogel & Welsch 2006). Recently, a simpler method using a standard CCD cameras was described, based on the first two moments of the recorded pixel-to-pixel photon fluctuation statistics (Matekole et al. 2020). Simplified, starlight is expected to produce a linear intensity-variance correlation, assuming that the (CCD) detector is linear in its response. Phase-squeezed (and anti-squeezed light) will however show a quadratic relation between intensity and variance (Figure 5). The effect is quite small with a quadratic coefficient of order 10^{-6} and thus requires the averaging of many photons. Still, an experiment using the existing CCD detectors on telescopes should be straightforward, because the squeezed-light test is performed using data analysis on the raw sensor data, without any need for additional equipment.

Squeezed light also exhibits second-order correlation effects as for bunched light. (For example, compare Figure 4 with Figure 2 in Wang & Fan 2012). However, I could not find any relevant practical work in this respect. Instead, it is more common to integrate the incoming flux over a certain time period and plot the photon number statistic, i.e., create a histogram of counted photons within this time (Breitenbach et al. 1997). Such a histogram can then be fit to a set of distributions e.g.,

using QuTiP (Johansson et al. 2013) for thermal and laser light, as well as various quantum states as shown in Figure 2.

5.8. Orbital angular momentum

Photons can carry a field spatial distribution in the form of orbital angular momentum (OAM). This degree of freedom can be used for quantum communications, such as secure direct communication (Li et al. 2020). For interstellar communication purposes, however, POAM is unattractive for two reasons.

First, it also occurs in many natural sources. The presence of astrophysical OAM has been shown using classical receivers on radio telescopes (Torner et al. 2005), detecting twisted light caused by the spin of the M87 black hole (Tamburini et al. 2020). Here, electromagnetic radiation is decomposed from the recorded voltage data into a set of discrete orthogonal eigenmodes. OAM has also been detected as a natural feature of optical starlight (Oesch & Sanchez 2014) and sunlight (Uribe-Patarroyo et al. 2011). An optical telescope is equipped with a vortex diffraction grating in front of the CCD, which produces three main OAM diffraction orders.

Second, interstellar distances are very large ($> 10^{16}$ m), so that the free space loss from diffraction, following the inverse square law, is very relevant. With OAM, the beam divergence increases even more, at least with the square root of the number of modes (Padgett et al. 2015; Padgett 2017). Figure 1 in Berkhou & Beijersbergen (2009) shows the difficulty in measuring spatially unresolved OAM: in the beam centre there is hardly any intensity, and off-axis there is hardly any phase change. Large apertures (or interferometers) are required to make measurements plausible in practice. In any case, using OAM reduces data rates over interstellar distances: beam divergence increases (flux decreases) with $\sqrt{1/M}$, while PIE increases only as $\log_2(1/M)$ bits per photon.

6. Conclusion and next steps

Some light from the heavens may be artificial in origin. It is worth exploring all signs of artificiality, including quantum properties. I propose to perform the following tests using available telescopes and equipment.

Squeezed light can be found with a CCD by measuring the first two moments of the recorded pixel-to-pixel photon fluctuation statistics (Matekole et al. 2020). A test for Fock states can be made by creating photon number statistic, i.e., creating a histogram of counted photons within this time (Breitenbach et al. 1997). Time-bin encoded qubits in the frequency domain can be seen as e.g., triplet spectral emission lines caused by the temporal modulation of the laser (Donohue et al. 2013). Alternatively, the events of high time-resolution photon counters (SNSPDs with ps timing) can be recorded (Gol’tsman et al. 2001; Prochazka et al. 2013), and searched for temporal correlations via data analysis such as Fourier transforms and autocorrelation tests.

Photon bunching can be found through the Hanbury Brown and Twiss effect (section 5.5) following the methods from Tan et al. (2014); Tan & Kurtsiefer (2017); Abeysekara et al. (2020). Experiments can use optical telescopes and VERITAS for stars like P Cygni, β Canis Majoris and ϵ Orioni. SNR calculations are provided by Saha (2019). A target list should include Helium white dwarfs (Fukugita 2020) and targets listed in Lacki et al. (2020).

The Hong-Ou-Mandel interference test (section 5.6) can be performed to search for indistinguishable photons. I propose to check the 100 brightest stars for artificial quantum signals, using twin telescopes with beamsplitters and photon counters.

Finally, coherence detecting systems of various types, like laser warners, should be pointed towards the stars. One example is the asymmetric Mach-Zehnder interferometer described by Benton (2019).

It may well be that a search dedicated for quantum signals is also sensitive to classical signals, e.g. in the form of a spread spectrum. The possibility of such a by-catch is not a valid argument against quantum SETI.

As quoted in the introduction, Giuseppe Cocconi proposed to search for radio signals because “photons per watt must be what counts”. This is correct for isotropic lighthouse-style beacons. For point-to-point communications in an interstellar network, however, tight beams at e.g., optical frequencies are preferred (Hippke & Forgan 2017; Hippke 2020). Then, the *number of bits per watt* must be what counts. These are maximized with *quantum communications*.

Following the SETI classification of Sheikh (2020), one important aspect of a potential ETI signal is its level of *ambiguity*, i.e. its potential to be a natural phenomenon unrelated to intelligent life. With quantum communications, a detection of Fock state photons or squeezed light would prove the artificiality of a signal, because there is no natural process which could create them. It is also straightforward to search for such signals, which is why we should start looking for them. They may offer the missing access link to an interstellar communication network.

References (127)

Aasi, J., Abadie, J., Abbott, B. P., et al. 2013, *Nature Photonics*, **7**, 613

Abbott, B. P., Abbott, R., Abbott, T. D., et al. 2016, *PhRvL*, **116**, 061102

Abeysekara, A. U., Archambault, S., Archer, A., et al. 2016, *ApJL*, **818**, L33

Abeysekara, A. U., Benbow, W., Brill, A., et al. 2020, *NatAs*, **4**, 1164

Ajagekar, A., & You, F. 2020, *arXiv*, arXiv:2003.00264. <https://arxiv.org/abs/2003.00264>

Arute, F., Arya, K., Babbush, R., et al. 2019, *Nature*, **574**, 505

Banaszek, K., Kunz, L., Jachura, M., & Jarzyna, M. 2020, *Journal of Lightwave Technology*, **38**, 2741

Barstow, M. A., & Holberg, J. B. 2007, *Extreme Ultraviolet Astronomy* (Cambridge University Press)

Bassi, A., & Ghirardi, G. 2008, *International Journal of Theoretical Physics*, **47**, 2500

Becerra, F. E., Fan, J., & Migdall, A. 2015, *Nature Photonics*, **9**, 48

Benedetti, M., Realpe-Gómez, J., Biswas, R., & Perdomo-Ortiz, A. 2016, *PhRvA*, **94**, 022308

Bennett, C., Shor, P., Smolin, J., & Thapliyal, A. 2002, *IEEE Transactions on Information Theory*, **48**, 2637

Bennett, C. H., & Wiesner, S. J. 1992, *PhRvL*, **69**, 2881

Benton, D. M. 2019, *PASP*, **131**, 074501

Benton, D. M., Zandi, M. A., & Sugden, K. 2019, *Proc. SPIE*, **11161**, 111610G

Berera, A. 2020, *PhRvD*, **102**, 063005

Berkhout, G. C. G., & Beijersbergen, M. W. 2009, *Journal of Optics A: Pure and Applied Optics*, **11**, 094021

Beskin, G., Borisov, N., Komarova, V., et al. 1997, *Astrophysics and Space Science*, **252**, 51

Bland-Hawthorn, J., Sellars, M., & Bartholomew, J. 2021, *arXiv*, arXiv:2103.07590. <https://arxiv.org/abs/2103.07590>

Blasone, M., Dell'Anno, F., DeSiena, S., & Illuminati, F. 2009, *EPL (Europhysics Letters)*, **85**, 50002

Breitenbach, G., Schiller, S., & Mlynek, J. 1997, *Nature*, **387**, 471

Brown, R. H., & Twiss, R. G. 1954, *Philosophical Magazine*, **45**, 663

Caleffi, M., Cacciapuoti, A. S., & Bianchi, G. 2018, *arXiv*, arXiv:1805.04360. <https://arxiv.org/abs/1805.04360>

Cline, E. 2015, *Armada* (Random House)

Cocconi, G., & Morrison, P. 1959, *Nature*, **184**, 844

Croke, S., Andersson, E., & Barnett, S. M. 2008, *PhRvA*, **77**, 012113

da Silva, M. P., Guha, S., & Dutton, Z. 2013, *PhRvA*, **87**, 052320

Deng, Y.-H., Wang, H., Ding, X., et al. 2019, *PhRvL*, **123**, 080401

Ding, D., Pavlichin, D. S., & Wilde, M. M. 2017, *arXiv*, arXiv:1705.08878. <https://arxiv.org/abs/1705.08878>

Dolinar, S. J. 1973, Research Laboratory of Electronics, MIT, *Quarterly Progress Report*, **11**, 115

Donohue, J. M., Agnew, M., Lavoie, J., & Resch, K. J. 2013, *PhRvL*, **111**, 153602

Eberhard, P. H., & Ross, R. R. 1989, *Foundations of Physics Letters*, **2**, 127

Fanizza, M., Rosati, M., Skotiniotis, M., et al. 2020, *arXiv*, arXiv:2006.06522. <https://arxiv.org/abs/2006.06522>

Fedrizzi, A., Ursin, R., Herbst, T., et al. 2009, *Nature Physics*, **5**, 389

Feynman, R. P. 1982, *International Journal of Theoretical Physics*, **21**, 467

Filatov, S., & Auzinsh, M. 2020, *arXiv*, arXiv:2001.08867. <https://arxiv.org/abs/2001.08867>

Forgan, D. H. 2014, *Journal of the British Interplanetary Society*, **67**, 232. <https://arxiv.org/abs/1410.7796>

Fukugita, M. 2020, 480

Gagatsos, C. N., Bullock, M. S., & Bash, B. A. 2020, *arXiv*, arXiv:2002.06733. <https://arxiv.org/abs/2002.06733>

Ghirardi, G., & Romano, R. 2012, *Journal of Physics A Mathematical General*, **45**, 232001

Gingerich, O. 2003, Interview of Philip Morrison by Owen Gingerich (American Institute of Physics, College Park, MD USA)

Giovannetti, V., Guha, S., Lloyd, S., et al. 2004, *PhRvL*, **92**, 027902

Giovannetti, V., Lloyd, S., & Maccone, L. 2006, *PhRvL*, **96**, 010401

Glauber, R. J. 1963, *Physical Review*, **131**, 2766

Gol'tsman, G. N., Okunev, O., Chulkova, G., et al. 2001, *Applied Physics Letters*, **79**, 705

Guerrini, S., Chiani, M., Win, M. Z., & Conti, A. 2019 (IEEE)

Guha, S. 2011, *PhRvL*, **106**, 240502

Guha, S., Zhuang, Q., & Bash, B. 2020, *arXiv*, arXiv:2001.03934. <https://arxiv.org/abs/2001.03934>

Hanbury Brown, R. 1956, *Nature*, **178**, 1046

Hanna, D. S., Ball, J., Covault, C. E., et al. 2009, *Astrobiology*, **9**, 345

Hao, S., Shi, H., Li, W., et al. 2021, *arXiv*, arXiv:2101.07482. <https://arxiv.org/abs/2101.07482>

Hausladen, P., Jozsa, R., Schumacher, B., et al. 1996, *Physical Review A*, **54**, 1869

Helstrom, C. W. 1976, *Quantum Detection and Estimation Theory*, Mathematics in Science and Engineering (Elsevier Science)

Hippke, M. 2018a, *Acta Astronautica*, **151**, 53

—. 2018b, *Journal of Astrophysics and Astronomy*, **39**, 74

—. 2019, *PASP*, **131**, 034502

—. 2020, *AJ*, **159**, 85

Hippke, M., & Forgan, D. H. 2017, *arXiv*, arXiv:1711.05761. <https://arxiv.org/abs/1711.05761>

Holevo, A. 1998, *IEEE Transactions on Information Theory*, **44**, 269

Holevo, A. S. 1973, Problemy Peredachi Informatsii, **9**, 3

Hong, C. K., Ou, Z. Y., & Mandel, L. 1987, *PhRvL*, **59**, 2044

Howard, A. W., Horowitz, P., Wilkinson, D. T., et al. 2004, *ApJ*, **613**, 1270

Jarzyna, M., Kuszaj, P., & Banaszek, K. 2015, *Optics Express*, **23**, 3170

Johansson, J. R., Nation, P. D., & Nori, F. 2013, *Computer Physics Communications*, **184**, 1234

Kimble, H. J. 2008, *Nature*, **453**, 1023

Kingsley, S. A. 1993, *Proc. SPIE*, **1867**, 75

Kipping, D., Frank, A., & Scharf, C. 2020, *International Journal of Astrobiology*, **19**, 430

Klimek, A., Jachura, M., Wasilewski, W., & Banaszek, K. 2016, *Journal of Modern Optics*, **63**, 2074

König, R., & Smith, G. 2013, *PhRvL*, **110**, 040501

Korpela, E. J., Anderson, D. P., Bankay, R., et al. 2011, *Proc. SPIE*, **8152**, 815212

Korzh, B., Zhao, Q.-Y., Allmaras, J. P., et al. 2020, *Nature Photonics*, **14**, 250

Kumar, S., Lauk, N., & Simon, C. 2019, *Quantum Science and Technology*, **4**, 045003

Lacki, B. C., Brzycki, B., Croft, S., et al. 2020, *arXiv*, arXiv:2006.11304. <https://arxiv.org/abs/2006.11304>

Leeb, W. R., Poppe, A., Hammel, E., et al. 2013, *Astrobiology*, **13**, 521

Li, L.-Y., Wang, T.-J., & Wang, C. 2020, *Modern Physics Letters B*, **34**, 2050017

Lloyd, S. 1996, *Science*, **273**, 1073

Lubin, P. 2016a, *Journal of the British Interplanetary Society*, **69**, 40. <https://arxiv.org/abs/1604.01356>

Lubin, P. 2016b, *Proc. SPIE*, **9981**, 99810H

Maiman, T. H. 1960, *Nature*, **187**, 493

Maire, J., Wright, S. A., Werthimer, D., et al. 2014, *Proc. SPIE*, **9147**, 91474K

Maire, J., Wright, S. A., Barrett, C. T., et al. 2019, *AJ*, **158**, 203

Mann, I., & Kimura, H. 2000, *JGR*, **105**, 10317

Manzalini, A. 2020, *Quantum Reports*, **2**, 221

Marcy, G. W. 2021, *arXiv*, arXiv:2102.01910. <https://arxiv.org/abs/2102.01910>

Matekole, E. S., Cuozzo, S. L., Prajapati, N., et al. 2020, *PhRvL*, **125**, 113602

Mead, C. C. 2013, PhD thesis, Harvard University

Merali, Z. 2016, *Science*, **352**, 1040

Müller, C. R., Seshadreesan, K. P., Peuntinger, C., & Marquardt, C. 2018, *arXiv*, arXiv:1811.09423. <https://arxiv.org/abs/1811.09423>

Oesch, D. W., & Sanchez, D. J. 2014, *A&A*, **567**, A114

Oi, D. K. L., Potoček, V., & Jeffers, J. 2013, *PhRvL*, **110**, 210504

Padgett, M. J. 2017, *Optics Express*, **25**, 11265

Padgett, M. J., Miatto, F. M., Lavery, M. P. J., et al. 2015, *New Journal of Physics*, **17**, 023011

Polyakov, S. V. 2013, *Single-Photon Generation and Detection - Physics and Applications. Series: Experimental Methods in the Physical Sciences*, **45**, 69

Popkin, G. 2017, *Nature*, **542**, 20

Price, D. C., Enriquez, J. E., Brzycki, B., et al. 2020, *AJ*, **159**, 86

Prochazka, I., Kodet, J., & Blazej, J. 2013, *Review of Scientific Instruments*, **84**, 046107

Reines, A. E., & Marcy, G. W. 2002, *PASP*, **114**, 416

Saglamyurek, E., Sinclair, N., Jin, J., et al. 2011, *Nature*, **469**, 512

Saha, P. 2019, *MNRAS*, **486**, 5400

Saleh, B., Teich, M., & John Wiley & Sons, L. 1991, Fundamentals of Photonics, Wiley Series in Pure and Applied Optics (Wiley)

Santana, T. S., Ma, Y., Malein, R. N. E., et al. 2017, *PhRvB*, **95**, 201410

Schnabel, R. 2017, *PhR*, **684**, 1

Schuetz, M., Vakoch, D. A., Shostak, S., & Richards, J. 2016, *ApJL*, **825**, L5

Schumacher, B., & Westmoreland, M. D. 1997, *PhRvA*, **56**, 131

Schwartz, R. N., & Townes, C. H. 1961, *Nature*, **190**, 205

Sheikh, S. Z. 2020, *International Journal of Astrobiology*, **19**, 237

Sheikh, S. Z., Siemion, A., Enriquez, J. E., et al. 2020, *AJ*, **160**, 29

Shvartsman, V. F. 1981, The MANIIa experiment and potentialities of the optical search for extraterrestrial civilizations (Goldberg, H. S. and Scadron, M. D.), **122**

Stancil, D. D., Adamson, P., Alania, M., et al. 2012, *Modern Physics Letters A*, **27**, 1250077

Stanton, R. H. 2019, *Acta Astronautica*, **156**, 92

Subotowicz, M. 1979, *Acta Astronautica*, **6**, 213

Tamburini, F., Thidé, B., & Della Valle, M. 2020, *MNRAS*, **492**, L22

Tan, P. K., & Kurtsiefer, C. 2017, *MNRAS*, **469**, 1617

Tan, P. K., Yeo, G. H., Poh, H. S., et al. 2014, *ApJL*, **789**, L10

Tellis, N. K., & Marcy, G. W. 2017, *AJ*, **153**, 251

Torner, L., Torres, J. P., & Carrasco, S. 2005, *Optics Express*, **13**, 873

Tosi, A., Mora, A. D., Zappa, F., & Cova, S. 2009, *Journal of Modern Optics*, **56**, 299

Uribe-Patarroyo, N., Alvarez-Herrero, A., López Ariste, A., et al. 2011, *A&A*, **526**, A56

Vogel, W., & Welsch, D. 2006, Quantum Optics (Wiley)

Vourdas, A., & da Rocha, J. 1994, *Journal of Modern Optics*, **41**, 2291

Wang, S., & Fan, H.-Y. 2012, *Journal of the Optical Society of America B Optical Physics*, **29**, 15

Wilde, M. M., Guha, S., Tan, S.-H., & Lloyd, S. 2012, *arXiv*, [arXiv:1202.0518](https://arxiv.org/abs/1202.0518). <https://arxiv.org/abs/1202.0518>

Wright, S. A., Drake, F., Stone, R. P., et al. 2001, *Proc. SPIE*, **4273**, 173

Wu, L.-A., Kimble, H. J., Hall, J. L., & Wu, H. 1986, *PhRvL*, **57**, 2520

Yang, M., Xu, F., Ren, J.-G., et al. 2019, *Optics Express*, **27**, 36114

Zhong, H.-S., Wang, H., Deng, Y.-H., et al. 2020, *Science*, **370**, 1460

Zhong, M., Hedges, M. P., Ahlefeldt, R. L., et al. 2015, *Nature*, **517**, 177